JOURNAL OF SOLID STATE CHEMISTRY 70, 71–81 (1987)

Molybdenum Cluster Chalcogenides Mo_6X_8: Electrochemical Intercalation of Closed Shell Ions Zn^{2+}, Cd^{2+}, and Na^{+}*

E. GOCKE, W. SCHRAMM, P. DOLSCHEID, AND R. SCHÖLLHORN†

Technische Universität Berlin, Institut für Anorganische Chemie, Strasse des 17. Juni 135, D-1000 Berlin 12, West Germany

Received December 29, 1986; in revised form March 13, 1987

The intercalation of d^{10} ions Zn^{2+} and Cd^{2+} by electron/ion transfer reactions into the Chevrel-type molybdenum cluster chalcogenides Mo_6X_8 (X = S, Se) demonstrates the competitive influence of electronic and steric factors upon these processes. The following rhombohedral phases have been identified: $Zn_1Mo_6S_8$, $Zn_2Mo_6S_8$, $Zn_1Mo_6Se_8$, $Zn_2Mo_6Se_8$, $Cd_1Mo_6S_8$, $Cd_1Mo_6Se_8$, and $Cd_2Mo_6Se_8$. Thermodynamic data and chemical diffusion coefficients are given. The intercalation of Na^+, which has an ionic radius close to that of Cd^{2+}, exhibits a strong influence of kinetics leading to the partial irreversibility of the reaction and the formation $Na_1Mo_6S_8$ and $Na_1Mo_6Se_8$, the first cubic phases among the molybdenum cluster chalcogenides $A_xMo_6X_8$.

Introduction

The rhombohedral molybdenum cluster chalcogenides Mo_6X_8 and $A_xMo_6X_8$ (X = S or Se) are known to exhibit extraordinary physical properties—in particular with respect to superconducting behavior—which depend strongly upon the nature of the chalcogen anion X, the nature of the ternary metal A, and the stoichiometry of the latter (*1*, *2*). The structure of the binary phases can be described by a framework matrix of interconnected Mo_6X_8 cluster units containing formally a system of intersecting "vacant channels" along the rhombohedral axes. It has been demonstrated that these structural characteristics as well as the specific electronic properties of these systems allow the reversible intercalation of guest cations up to a critical size into the Mo_6X_8 matrix at ambient temperature via electron/ion transfer (*3*, *4*). These reactions are most interesting, since they open the way to (i) the synthesis of new metastable ternary and quaternary phases not accessible by thermal preparation and (ii) the reversible modification of the physical properties of the host matrix via chemical reactions at ambient temperature. A most fascinating phenomenon is the observation that even bivalent transition metal ions can be intercalated reversibly into the Mo_6X_8 matrix (*4*, *5*); according to our knowledge the resulting phases are the only known representatives of transition metal ionic conductors at room temperature so far. We report here on the formation and properties of ternary phases with transition metal ions having d^{10} configuration $Zn_xMo_6X_8$ and $Cd_xMo_6X_8$ which have not been studied in detail so far. Since Cd^{2+} turned out to be

* Dedicated to Franz Jellinek.

† To whom correspondence should be addressed.

0022-4596/87 $3.00

close to the critical radius for intercalation with respect to its size, we extended our investigations on the monovalent s^0 ion Na^+ which formally has an ionic radius closely similar to Cd^{2+} in order to compare the influence of cation size and charge on the critical radius and on the maximum stoichiometry x which itself is governed by electronic as well as by steric aspects.

Experimental

The binary phases Mo_6S_8 and Mo_6Se_8 were prepared from the ternary compounds $Cu_2Mo_6X_8$ which had been obtained by heating stoichiometric amounts of the elements in sealed quartz ampoules at 1150°C for 4 days and subsequent slow cooling to room temperature. Rhombohedral lattice parameters of the Cu phases agreed with literature data (*1*). Anodic oxidation of the latter in 0.1 *N* H_2SO_4 leads to quantitative removal of Cu under formation of Mo_6S_8 and Mo_6Se_8 (lattice parameters given in Table I). Galvanostatic titration, potentiostatic reaction with integration of the charge consumed, slow voltammetry and cyclic voltammetry, short circuit runs, and EMF measurements (equilibrium potentials) were used for the electrochemical study of the reactions (300 K). The working electrodes consisted of polycrystalline pressed samples. In the case of the Na/Mo_6S_8 system 1% wt of Teflon was added as binder; in the absence of Teflon the mechanical stress due to the strong increase in unit cell volume leads to regions that loose electronic contact and thus to significant errors in the values for the electrochemical charge transfer.

Dried salts of analytical purity ($Zn(ClO_4)_2$, $Cd(ClO_4)_2$, and $NaClO_4$) in high-purity dry acetonitrile or propylene carbonate, respectively, served as aprotic electrolytes. Reactions with Zn^{2+} and Cd^{2+} were also performed in aqueous electrolytes. For comparison purposes $Na_3Mo_6S_8$ samples were prepared in addition by reaction of Mo_6S_8 with Na metal dissolved in liquid NH_3 at −30°C. All operations were carried out in inert gas atmosphere.

For the evaluation of the chemical diffusion coefficients the galvanostatic intermittent titration technique (GITT) was applied (*6*). Wet analysis, atomic absorption spectrometry, and microanalysis were used for

TABLE I

LATTICE PARAMETERS AND UNIT CELL VOLUMES OF BINARY AND TERNARY MOLYBDENUM CLUSTER CHALCOGENIDES Mo_6X_8 AND $A_xMo_6X_8$

Compound	A	x	X	a_R (pm)	α_R (°)	$V_R \times 10^6$ (pm^3)	a_H (pm)	c_H (pm)	c/a	$V_H \times 10^6$ (pm^3)
Mo_6S_8	—	—	S	643.0	91.27	266.0	919.2	1088.9	1.1846	796.7
Mo_6Se_8	—	—	Se	666.0	91.70	294.9	955.5	1119.6	1.1717	885.2
$Zn_1Mo_6S_8$	Zn	1	S	648.1	94.56	269.5	952.4	1029.4	1.0808	808.6
$Zn_2Mo_6S_8$	Zn	2	S	648.6	94.58	270.1	953.3	1028.2	1.0786	809.2
$Zn_1Mo_6Se_8$	Zn	1	Se	673.7	94.46	302.9	990.3	1071.2	1.0817	909.7
$Zn_2Mo_6Se_8$	Zn	2	Se	683.6	94.69	316.1	1005.3	1082.4	1.0767	947.2
$Cd_1Mo_6S_8$	Cd	1	S	651.7	92.77	276.0	943.7	1072.9	1.1369	827.8
$Cd_1Mo_6Se_8$	Cd	1	Se	675.7	92.53	307.5	976.5	1117.8	1.1447	923.1
$Cd_2Mo_6Se_8$	Cd	2	Se	683.2	95.25	328.7	1025.0	1084.0	1.0576	986.3
$Na_1Mo_6S_8$	Na	1	S	650.7	90.00	275.5	923.1	1132.1	1.2264	828.7
$Na_3Mo_6S_8$	Na	3	S	673.3	94.57	302.1	989.7	1072.5	1.0837	909.8
$Na_1Mo_6Se_8$	Na	1	Se	676.5	90.00	309.5	956.6	1172.2	1.2254	929.0

Note. R = rhombohedral, H = hexagonal.

analytical determination of the composition of products. X-ray powder data were obtained from samples in sealed borosilicate glass capillaries by the Simon–Guinier technique. Critical temperatures T_c for the transition normal conductivity/superconductivity have been measured by the AC susceptibility technique (Meissner effect).

Results and Discussion

Zn/Mo₆S₈

The reactions of Mo_6S_8 electrodes with Zn^{2+} ions had been originally performed by us in aqueous galvanic cells of the type

$$Zn\|Zn^{2+},\ H_2O\|Mo_6S_8.$$

It turned out that the aqueous cells presented some specific problems so that the experiments had to be carried out in aprotic electrolytes:

$$Zn\|Zn^{2+},\ CH_3CN\|Mo_6S_8.$$

We shall first describe here the results obtained in the acetonitrile electrolyte and thereafter discuss the problems encountered with aqueous electrolyte solutions.

Figure 1a presents the potential/charge transfer diagram obtained on galvanostatic cathodic reduction of Mo_6S_8 in Zn^{2+}/CH_3CN at low current density. It is clearly seen that the reaction is terminated after an electrochemical charge transfer of $n = 4$ (e^-/Mo_6S_8), where a sharp potential step indicates the transition to Zn metal deposition. The potential step at $n = 2$ separates two potential plateau regions. The first region indicated as I in Fig. 1a should correspond to a two-phase system, since the potential remains constant; i.e., $\Delta_R G$ = constant. This conclusion is verified by the structural data given in Fig. 1b which confirm the coexistence of the two phases of Mo_6S_8 and a ternary phase with the analytical composition $Zn_\iota Mo_6S_8$. The chemical reaction proceeding in region I can thus be

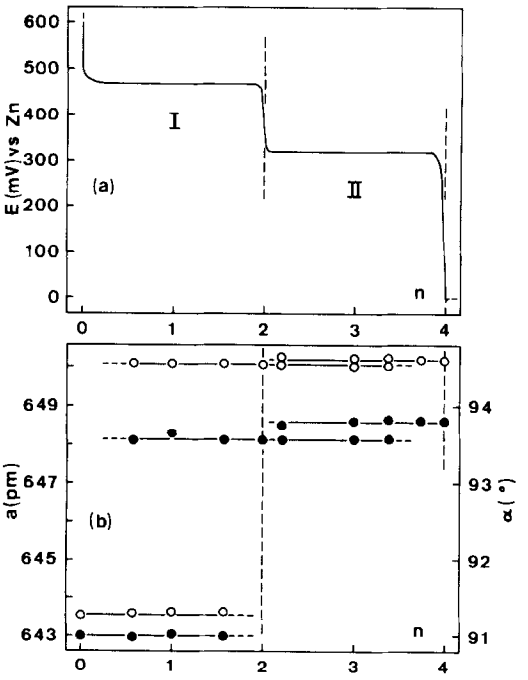

FIG. 1. Formation of $Zn_xMo_6S_8$ by galvanostatic cathodic reduction of Mo_6S_8 in aprotic Zn^{2+} electrolyte (2 *M* $Zn(ClO_4)_2/CH_3CN$) at 300 K. (a) Change of potential *E* (vs Zn^0/Zn^{2+}) of the working electrode with the charge transfer *n* (e^-/Mo_6S_8) and (b) change of the rhombohedral lattice parameters with *n* (a_R = ●, α_R = ○).

described by Eq. (1). Similarly, the second region II is a two-phase system

$$Zn^{2+} + 2e^- + Mo_6S_8 \rightleftharpoons Zn_\iota Mo_6S_8 \quad (1)$$

with the coexisting phases $Zn_\iota Mo_6S_8$ and $Zn_2Mo_6S_8$ (Figs. 1a, 1b); the reaction can be described by

$$Zn^{2+} + 2e^- + Zn_\iota Mo_6S_8 \rightleftharpoons Zn_2Mo_6S_8. \quad (2)$$

The integral analytical Zn content $\bar{x}$ of samples collected at given *n* values corresponds linearly with the charge transfer according to $\bar{x} = n/2$; i.e., no side reactions occur. The process is fully reversible; on anodic oxidation of $Zn_2Mo_6S_8$ the compounds $Zn_\iota Mo_6S_8$ and Mo_6S_8 appear again. According to the X-ray data (lattice parameters given in Table I) the two zinc compounds are line

TABLE II

FREE ENERGIES OF FORMATION ($\Delta_R G$) AND CORRESPONDING EMF VALUES FOR TERNARY MOLYBDENUM CLUSTER CHALCOGENIDES $A_xMo_6X_8$

A	X	Reaction	$\Delta_R G$ (kJ/mole)	EMF (V)
Zn	S	$Zn + Mo_6S_8 \rightleftarrows Zn_1Mo_6S_8$	−91.7	0.475
Zn	S	$Zn + Zn_1Mo_6S_8 \rightleftarrows Zn_2Mo_6S_8$	−63.3	0.328
Zn	S	$2Zn + Mo_6S_8 \rightleftarrows Zn_2Mo_6S_8$	−155.0	—
Zn	Se	$Zn + Mo_6Se_8 \rightleftarrows Zn_1Mo_6Se_8$	−73.5	0.381
Zn	Se	$Zn + Zn_1Mo_6Se_8 \rightleftarrows Zn_2Mo_6Se_8$	−67.2	0.348
Zn	Se	$2Zn + Mo_6Se_8 \rightleftarrows Zn_2Mo_6Se_8$	−140.7	—
Cd	S	$Cd + Mo_6S_8 \rightleftarrows Cd_1Mo_6S_8$	−21.2	0.110
Cd	Se	$Cd + Mo_6Se_8 \rightleftarrows Cd_1Mo_6Se_8$	−66.2	0.343
Cd	Se	$Cd + Cd_1Mo_6Se_8 \rightleftarrows Cd_2Mo_6Se_8$	−34.4	0.178
Cd	Se	$2Cd + Mo_6Se_8 \rightleftarrows Cd_2Mo_6Se_8$	−100.6	—
Na	S	$3Na + Mo_6S_8 \rightarrow Na_3Mo_6S_8$	−432.5	1.494

phases. Galvanostatic cycling and combined potentiostatic/galvanostatic measurements suggest a rather small phase width of 0.97–1.03 for $Zn_1Mo_6S_8$ and 1.90–2.00 for $Zn_2Mo_6S_8$. The free energies of the reactions represented by Eqs. (1) and (2) are listed in Table II along with the equilibrium potentials. Chemical diffusion coefficients for both phases are given in Table III.

Basically the results in aqueous electrolytes were found to be identical to those found with aprotic electrolytes. It turned out, however, that the ternary Zn phases decompose slowly in water under final formation of Mo_6S_8 and H_2 (Eq. (3)):

$$Zn_xMo_6S_8 + 2x\ H_2O \rightarrow Mo_6S_8 + xH_2 + xZn(OH)_2. \quad (3)$$

Due to this slow side reaction, the overall electrochemical charge transfer values become larger; also an additional "ghost region" appears before the potential of Zn deposition is reached. Similarly, on reoxidation of the terminal phase the charge yield is severely reduced in aqueous electrolytes.

Although the change in potential and in $\Delta_R G$ from $Zn_1Mo_6S_8$ to $Zn_2Mo_6S_8$ is significant (Table II), the change in lattice parameters (Table I) is unusually small. The rhombohedral lattice parameters of $Zn_1Mo_6S_8$ agree well with those reported for a phase with the composition $Zn_{1.1}Mo_6S_8$ prepared thermally from the elements (7). $Zn_2Mo_6S_8$ is a new metastable compound that cannot be obtained by thermal preparation and which undergoes decomposition upon heating at higher temperatures to products that have not been identified. The increase in unit cell volume (0.2%, Table I) is again very small on going from Zn_1 to Zn_2. This is illustrated in Fig. 2a which gives a comparison of unit cell volumes for a series of ternary sulfides $A_xMo_6S_8$ with mono- and bivalent guest cat-

TABLE III

CHEMICAL DIFFUSION COEFFICIENTS $\tilde{D}$ OF TERNARY PHASES $Zn_xMo_6X_8$ AT 300 K (PREPARED VIA ELECTROCHEMICAL INTERCALATION IN APROTIC ELECTROLYTES)

Compound	$\tilde{D}$ (cm^2 s^{-1})
$Zn_1Mo_6S_8$	1.5×10^{-9}
$Zn_2Mo_6S_8$	4.5×10^{-10}
$Zn_1Mo_6Se_8$	5.9×10^{-8}
$Zn_2Mo_6Se_8$	3.0×10^{-8}

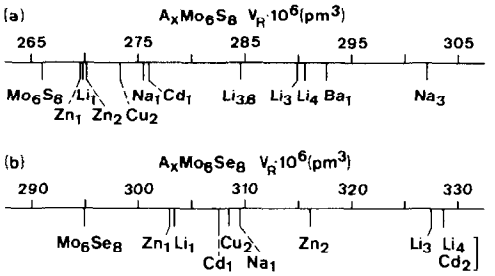

FIG. 2. Comparison of rhombohedral unit cell volumes of ternary molybdenum cluster chalcogenides. (a) $A_xMo_6S_8$, and (b) $A_xMo_6Se_8$.

ions. The rather small change in unit cell volume seems to be characteristic for phases $A_1Mo_6S_8/A_2Mo_6S_8$ with small bivalent guest cations and has also been described recently for $Ni_1Mo_6S_8$ and $Ni_2Mo_6S_8$, where the change amounts to only 0.5% (*8*).

Band structure calculations (*9*, *10*) as well as the ionic structure model (*2*) predict in electronic terms a maximum possible uptake of $4e^-$ per Mo_6S_8 unit, if a rigid band structure is assumed. Since the number of vacant sites along the "channels" is rather high and the ionic radius of Zn^{2+} is rather small (74 pm), the terminal product stoichiometry expected is $Zn_2Mo_6S_8$ with a charge transfer of $4e^-/Mo_6S_8$. This is in fact observed formally, if Eqs. (1) and (2) correspond to a quantitative transfer of the electrons to the host lattice matrix. The complete occupation of the upper band with four electrons must result in a metal/semiconductor transition (*1*). Earlier measurements by us have shown, however, that both compounds Zn_1 and Zn_2 become superconducting at 3.3 and 3.1 K, respectively (*11*). Literature data report a transition temperature of 3.6 K for the thermal phase $Zn_{1.1}Mo_6S_8$ (*12*). An explanation of the superconducting properties of $Zn_2Mo_6S_8$ has been suggested on the basis of a model with partial charge transfer to the host matrix, i.e., covalent bonding between the guest metal cations (*4*, *13*). We have thus two potential models, I and II, for the electron distribution:

I $(Zn^{2+})_2[Mo_6S_8]^{4-}$ semiconductor

II $(^+Zn\text{–}Zn^+)[Mo_6S_8]^{2-}$ metal/superconductor

The extremely small unit cell volume change could be explained by the assumption that $Zn_1Mo_6S_8$ is to be formulated similarly by $(^+Zn\text{–}Zn^+)_{1/2}[Mo_6S_8]^-$ with $(Zn\text{–}Zn)^{2+}$ units occupying half of the unit cells, so that filling of the residual vacant unit cells to $Zn_2Mo_6S_8$ would result in a minor volume change only.

The original data for the transition temperatures of Zn_1 and Zn_2 phases were obtained from samples prepared from aqueous electrolytes. We have repeated these experiments under identical conditions; the data observed confirm the earlier measurements. Additional investigations on samples of Zn_1 and Zn_2 prepared in aprotic electrolytes showed, however, no superconducting transition down to 1.5 K, the limit of our equipment. Preliminary ^1H-NMR studies confirmed the presence of small amounts of protons in samples prepared in aqueous electrolytes. It is obvious therefore that cointercalation of protons strongly affects the physical properties of these phases and that the electron transfer problem cannot thus be solved at present with the available data.

Zn/Mo₆Se₈

The potential/charge transfer diagram for the cathodic reduction of Mo_6Se_8 in galvanic cells with aprotic electrolytes $Zn\|Zn^{2+}$, $CH_3CN\|Mo_6Se_8$ is given in Fig. 3a. The shape of the curve is closely similar to that for the sulfide system Zn/Mo_6S_8. The X-ray data (Fig. 3b) confirm the existence of two two-phase regions, I and II, with the coexisting phases $Mo_6Se_8/Zn_1Mo_6Se_8$ and $Zn_1Mo_6Se_8/Zn_2Mo_6Se_8$ according to Eqs. (4) and (5).

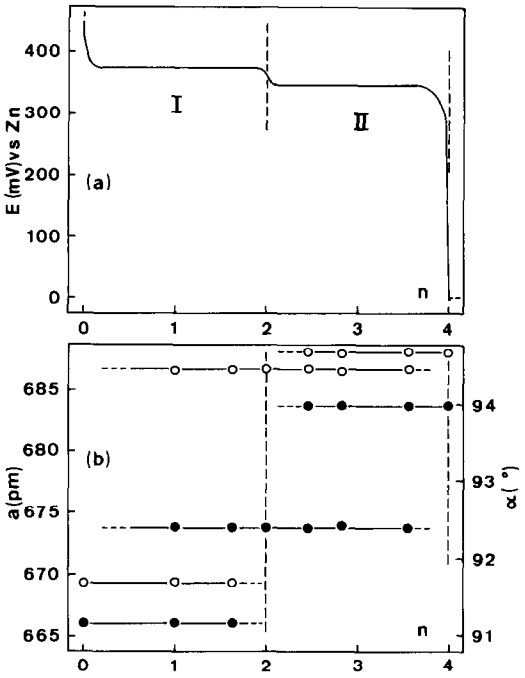

FIG. 3. Formation of $Zn_xMo_6Se_8$ by galvanostatic cathodic reduction of Mo_6Se_8 in aprotic Zn^{2+} electrolyte. (a) Change of potential E with the charge transfer n, and (b) change of rhombohedral lattice parameters with n (a_R = ●, α_R = ○).

$$Zn^{2+} + 2e^- + Mo_6Se_8 \rightleftharpoons Zn_1Mo_6Se_8 \quad (4)$$

$$Zn^{2+} + 2e^- + Zn_1Mo_6Se_8 \rightleftharpoons Zn_2Mo_6Se_8. \quad (5)$$

Analytical data prove a clear correlation of the integral Zn content $\bar{x}$ with the electrochemical charge transfer n according to $\bar{x} = n/2$. The phase width of $Zn_1Mo_6Se_8$ as determined electrochemically (cycling experiments) amounts to $z = 0.06$ in $Zn_{1\pm z}Mo_6Se_8$. In contrast with the sulfide system the change in $\Delta_R G$ from $Zn_1Mo_6Se_8$ to $Zn_2Mo_6Se_8$ is rather small (Table II), but the changes in unit cell volume (4.3%, Fig. 2b) and in the lattice parameter a_R (Table I) are quite significant. The lattice distortion as expressed by the changes in α_R and c/a is much smaller, however, as compared to the sulfide system (Table I).

Earlier cyclic voltammetry investigations by us on the Zn/Mo_6S_8 system demonstrated a rather high ionic mobility of Zn ions in the Mo/S framework (*5*). We have now measured the chemical diffusion coefficients for the zinc sulfide and selenide phases by the galvanostatic intermittent titration technique (*6*). The values obtained are given in Table III. They confirm the relatively high mobility of Zn ions at 300 K; the change of $\tilde{D}$ with the stoichiometry is rather small. Closely similar values for $\tilde{D}$ have been observed by us recently for the Ni/Mo_6S_8 system (*8*). One would expect in fact a rather high activation energy for the site change of cations with a high charge/radius ratio such as Zn^{2+} or Ni^{2+}. An explanation of the unusually high mobility of small transition metal ions in the Mo_6X_8 framework has been suggested recently (*4, 13, 14*). It was assumed either that these ions are formally monovalent as discussed above (partial charge transfer) or that an equilibrium exists with a small fraction of the metal ions being monovalent and a rapid electron transfer via the Mo_6X_8 matrix, $A^{2+} + e^- \rightleftharpoons A^+$.

Measurements of the diffusion coefficients of $Zn_xMo_6X_8$ phases in aqueous electrolytes yielded values that were two orders of magnitude higher than those obtained in aprotic electrolyte systems. This discrepancy is attributed to the cointercalation of protons under those conditions which exhibit far higher mobilities as compared to Zn^{2+}. The same phenomenon has been observed in the Ni/Mo_6S_8 system, where nonstoichiometric hydrogen bronzes Ni_xH_y Mo_6S_8 could be identified (*8*).

Cd/Mo₆X₈

The critical radius for the intercalation of guest ions in Mo_6X_8 systems must be below ~100 pm, since rare-earth ions with hard sphere radii of ~100–110 pm cannot be intercalated into the binary phases or deintercalated from ternary phases prepared by

thermal reaction. The ionic radius of Cd^{2+} (97 pm) is ca. 30% greater as compared to the radius of Zn^{2+} and should be close to the critical radius. It is clear that under these circumstances, small differences in the size of the available lattice sites must become of influence, i.e., differences between the lattice parameters of the sulfide and the selenide host matrix. This is in fact what we observed. The intercalation of Cd^{2+} in aqueous electrolytes into Mo_6S_8 leads to a maximum charge transfer $n = 2$ (e^-/Mo_6S_8) consistent with the formation of the line phase $Cd_1Mo_6S_8$. Figure 4a shows a clear two-phase system $Mo_6S_8/Cd_1Mo_6S_8$

$$Cd^{2+} + 2e^- + Mo_6S_8 \rightleftharpoons Cd_1Mo_6S_8, \quad (6)$$

which is confirmed by the structural data given in Fig. 4b. Cyclic voltammetry studies showed similarly only a single peak, before the potential of Cd metal deposition is reached. Potentiostatic measurements of the charge transfer are also in agreement with a value of $n = 2$. The lattice parameters of $Cd_1Mo_6S_8$ (Table I) are in accordance with those given in the literature for a phase $Cd_{1.1}Mo_6S_8$ obtained by thermal preparation from the elements (*7*). The strong influence of kinetics upon the reaction as indicated by the strong variation in apparent potential with the current density is obviously due to the lower mobility of the large Cd ions in the Mo_6S_8 framework; diffusion coefficients for Cd could not therefore be measured with reliable accuracy by electrochemical methods. The critical temperature for superconduction was $T_c = 2.1$ K; this value is in agreement with the data reported in the literature for $Cd_{1.1}Mo_6S_8$ prepared from the elements (*1*). The Cd/Mo_6S_8 system clearly demonstrates the competing influence of electronic and steric factors. While band structure considerations only would predict a terminal composition $Cd_2Mo_6S_8$, the composition found in reality seems to be limited by steric aspects. The lattice distortion as indicated by the rhombohedral angle α_R is much less as compared to the Zn phases and Cd behaves in the Mo_6S_8 lattice more like a "large ion" in terms of the classification given by Yvon (*2*). It is likely thus that the position of Cd ions in $Cd_1Mo_6S_8$ is close to the unit cell origin, like in $In_1Mo_6S_8$ which has a closely similar α_R value of 93° (*2*).

"Normal" behavior is encountered again in the selenide system. The larger anions lead to more favorable dimensions of the vacant sites and the system is thus able to intercalate two Cd ions corresponding to a maximum charge transfer of $n = 4$. Electrochemical, structural, and thermodynamic data are given in Fig. 5 and Tables I and II. Again two two-phase regions as described by

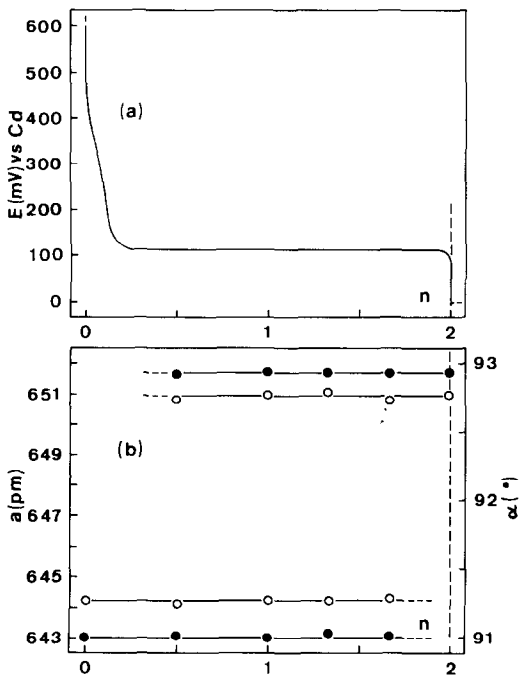

FIG. 4. Formation of $Cd_xMo_6S_8$ by galvanostatic cathodic reduction of Mo_6S_8 in aqueous Cd^{2+} electrolyte (2 *M* $CdSO_4$). (a) Change of potential *E* (vs Cd^0/Cd^{2+}) with the charge transfer *n*, and (b) change of rhombohedral lattice parameters with *n* (a_R = ●, α_R = ○).

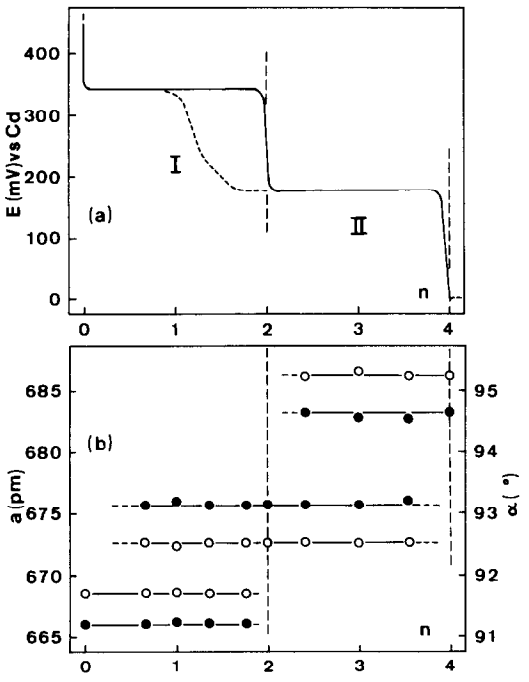

FIG. 5. Formation of $Cd_xMo_6Se_8$ by galvanostatic cathodic reduction of Mo_6Se_8 in aqueous Cd^{2+} electrolyte. (a) Change of potential E with the charge transfer n, and (b) change of rhombohedral lattice parameters with n (a_R = ●, α_R = ○); dashed line refers to primary reduction.

$$Cd^{2+} + 2e^- + Mo_6Se_8 \rightleftharpoons Cd_1Mo_6Se_8 \quad (7)$$

$$Cd^{2+} + 2e^- + Cd_1Mo_6Se_8 \rightleftharpoons Cd_2Mo_6Se_8 \quad (8)$$

are observed. The influence of kinetics is still clearly visible, however. The first reduction curve shows a strong deviation from the equilibrium potential in the range of $n = 1$ to $n = 2$, which disappears on further oxidation/reduction cycling. $Cd_2Mo_6Se_8$ is a new metastable phase which decomposes at elevated temperatures; $Cd_1Mo_6Se_8$ exhibits lattice parameters closely similar to those given in the literature for a thermal phase with the composition $Cd_{1.2}Mo_6Se_8$ (*1*). In agreement with the classification of Cd ions as "large" cations the unit cell volume change $Mo_6Se_8/Cd_1Mo_6Se_8/Cd_2Mo_6Se_8$ is rather large (Fig. 2b).

Na/Mo₆S₈

The interesting influence of steric parameters upon the reactivity of Cd^{2+} ions with the Mo_6X_8 chalcogenides led us to investigate the reactivity of the host lattices with sodium cations, since Na^+ has an ionic radius of 95 pm, which is closely similar to that of Cd^{2+}. Since sodium is monovalent, a terminal stoichiometry of $Na_4Mo_6S_8$ is to be expected under electronic aspects; the large ionic radius of Na^+ might in terms, however, induce steric restraints for the insertion of a large number of these ions.

The reactions were performed in galvanic cells $Na\|Na^+$, propylene carbonate$\|$ Mo_6S_8 with sodium metal as counter and reference electrodes. Figure 6a shows the potential/charge transfer diagram for this reaction. After a transfer of $4e^-/Mo_6S_8$ the potential of Na deposition is reached and analytical data confirm that an uptake of $4Na^+$ is in fact observed ($\bar{x} = n$). The reaction exhibits a severe influence of kinetics which leads to an unexpected kind of partial reversibility of the process. As illustrated in Fig. 6a the cathodic reduction shows a potential plateau in region I up to $n = 3$. Structural data prove the coexistence of Mo_6S_8 and a sodium phase $Na_3Mo_6S_8$. This transition is related to the largest change in unit cell volume observed so far for the $A_xMo_6X_8$ cluster chalcogenides (13.6%, cf. Figs. 6b and 2a and Table I). Further reduction (region II) leads to the terminal phase $Na_4Mo_6S_8$. This reaction does not proceed, however, at the equilibrium potential and strong line broadening is observed in the X-ray pattern. Both factors are responsible for the fact that a clear decision between a two-phase system and a one-phase system is not possible in this region. There is evidence that partially irreversible decomposition accompanies the reaction in region II.

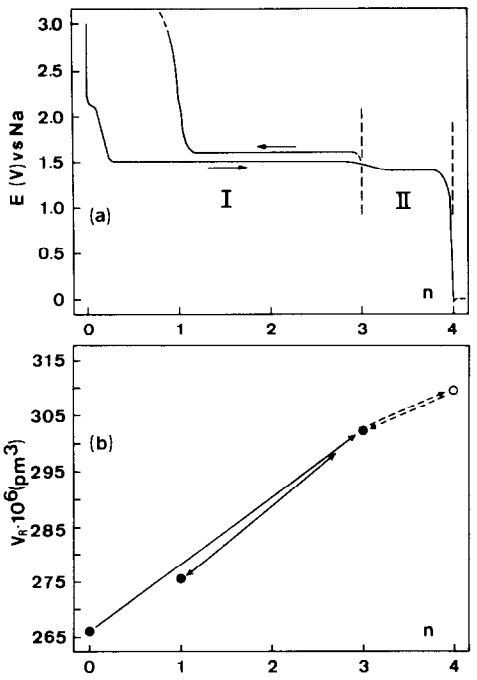

FIG. 6. $Na_xMo_6S_8$: (a) Potential/charge transfer diagram indicating a reduction/oxidation cycle, and (b) diagram illustrating the change in rhombohedral cell volume in the course of a reduction/oxidation cycle.

The reaction was found to be fully reversible only in the limited range of $n = 1$ to $n = 3$ (referring to the abscissa given in Fig. 6a). On reoxidation of $Na_3Mo_6S_8$ a newly defined metastable phase is formed after a transfer of $2e^-/Na_3Mo_6S_8$ with the idealized composition $Na_1Mo_6S_8$ (two-phase system) which cannot be further oxidized under the conditions applied to Mo_6S_8 but can be reduced again to $Na_3Mo_6S_8$. The reactions observed can be described thus by Eqs. (9)–(11).

$$3\,Na^+ + 3e^- + Mo_6S_8 \rightarrow Na_3Mo_6S_8 \quad (9)$$

$$Na^+ + e^- + Na_3Mo_6S_8 \rightleftharpoons Na_4Mo_6S_8 \quad (10)$$

$$Na_3Mo_6S_8 \rightleftharpoons 2\,Na^+ + 2e^- + Na_1Mo_6S_8. \quad (11)$$

While $Na_3Mo_6S_8$ and $Na_4Mo_6S_8$ are—as expected–strongly susceptible to air and moisture, the phase $Na_1Mo_6S_8$ is completely stable in air and water and even after a storage of one year under H_2O no change in composition or X-ray pattern could be observed. Larger amounts of this phase have been prepared by us via chemical intercalation of Mo_6S_8 by Na metal dissolved in liquid ammonia at −30°C in a ratio $Na/Mo_6S_8 = 3$. The resulting compound $Na_3Mo_6S_8$ was transformed to $Na_1Mo_6S_8$ either by reaction with an aqueous ethanol solution or by reaction with J_2/CH_3CN. Small numbers of protons have been observed in $Na_1Mo_6S_8$ by microanalysis and ^{1}H-NMR, if the oxidation reaction is carried out in protolytic solvents. The exact analytical composition of the phase obtained by oxidation in aprotic solvents varies slightly between $Na_{1.05}Mo_6S_8$ and $Na_{1.1}Mo_6S_8$. Mo_6S_8 can be obtained again, however, from $Na_1Mo_6S_8$, e.g., by reduction in aprotic Li^+ or Zn^{2+} electrolyte (until the potential of metal deposition has been reached) and subsequent anodic reoxidation.

A further unusual phenomenon is the fact that $Na_1Mo_6S_8$ can be indexed with a cubic lattice parameter of 650.7 pm (Table I); it is the only cubic phase observed so far among the $A_xMo_6X_8$ compounds. $Na_1Mo_6S_8$ with $\alpha_R = 90°$ should correspond therefore formally to the category of compounds with "large" ternary atoms like $PbMo_6S_8$ and $SnMo_6S_8$ which exhibit rhombohedral angles rather close to 90°. In the latter compounds the ternary atoms are located exactly at the unit cell origin and are immobile (*1*). The sodium ions in $Na_1Mo_6S_8$ are obviously similarly immobile and we assume that Na is located also at the unit cell origin. The lack of Na^+ transport in this phase is responsible for the fact that $Na_1Mo_6S_8$ cannot be oxidized to Mo_6S_8. The absence of Na^+ transport in the cubic phase also prevents the formation of this compound on reduction of Mo_6S_8. $Na_1Mo_6S_8$ can be formed, however, from $Na_3Mo_6S_8$—which has an extremely high unit cell volume (Fig.

6b)—by oxidation under volume contraction. The microscopic mechanism of the reaction, which proceeds in a two-phase system, is hard to understand in terms of Na^+ transport since the Na^+ atoms in the newly formed Na_I phase are immobile and are blocking Na^+ transport. We found, however, by electron microscopy studies that upon formation of $Na_3Mo_6S_8$ due to the strong volume increase and resulting lattice strain the crystallite size is severely reduced and diffusion lengths for the oxidation reaction are thus strongly diminished. It is conceivable that in the course of the oxidation process (Eq. (11)) small domains of $Na_3Mo_6S_8$ remain isolated in terms of Na^+ transport by the surrounding Na_I Mo_6S_8 phase formed which would explain in a kinetic model that the ideal stoichiometry $Na_IMo_6S_8$ cannot be attained quantitatively. The mechanism of the inverse pathway $Na_I \rightarrow Na_3$ does not provide similar problems since the new phase Na_3 growing at the interphase boundary is an ionic conductor.

Preliminary investigations on the intercalation of Na^+ into Mo_6Se_8 demonstrated that the reactivity of the selenide is closely similar to that of the sulfide. Reoxidation of rhombohedral $Na_3Mo_6Se_8$ yields cubic $Na_IMo_6Se_8$ (Table I) which is metastable but kinetically inert with respect to further oxidation to Mo_6Se_8.

Conclusions

The molybdenum cluster chalcogenides $Mo_6X_8/A_xMo_6X_8$ are quite obviously highly interesting model systems for a systematic investigation of the correlations between composition, structure, physical properties, and chemical reactivity of solid systems. The results of the present study demonstrate the competition between electronic and steric factors as well as the influence of kinetics upon the topotactic reactivity of Mo_6X_8 at low temperatures. The value of the qualitative models used for discussion of the experimental facts is limited, however. It can be understood, e.g., that upon oxidation of $Na_3Mo_6S_8$ one of the sodium ions falls into a combined energetic/steric trap and simulates the behavior of a "large" cation with the consequence of a rigid lattice position and blocked sodium transport. It is not clear on the other hand why even Mo_6S_8 is able to take up four sodium ions with a significant negative free enthalpy of formation, while the ionic radius of Na^+ is close to the critical radius for intercalation. Similarly, the validity of models proposed for describing the phenomenon of transition metal ion conductivity at ambient temperature cannot be evaluated at present. Major contributions for a better understanding of the systems under discussion should be expected from refined structural data which are not easy to obtain, however, since the reaction products are usually polycrystalline phases.

References

1. Ø. FISCHER AND M. B. MAPLE (Eds.), "Superconductivity in Ternary Compounds," Vols. I and II, Springer-Verlag, Berlin/Boston (1982).
2. K. YVON, *in* "Current Topics in Materials Science" (E. Kaldis, Ed.), Vol. II, p. 53, North-Holland, Amsterdam (1979).
3. R. SCHÖLLHORN, *Angew. Chem.* **92,** 1015 (1980), *Angew. Chem. Int. Ed. Engl.* **19,** 983 (1980).
4. R. SCHÖLLHORN, *in* "Inclusion Compounds" (J. L. Atwood, J. E. D. Davies, and D. D. Mac Nicol, Eds.), Vol. I, p. 249, Academic Press, London/New York (1984).
5. R. SCHÖLLHORN, M. KÜMPERS, AND J. O. BESENHARD, *Mater. Res. Bull.* **12,** 781 (1977).
6. W. WEPPNER AND R. A. HUGGINS, *Annu. Rev. Mater. Sci.* **8,** 269 (1978).
7. R. CHEVREL, M. SERGENT, AND J. PRIGENT, *J. Solid State Chem.* **3,** 515 (1971); R. Chevrel, thèse, Université de Rennes (1974).
8. W. SCHRAMM, E. GOCKE, AND R. SCHÖLLHORN, *Mater. Res. Bull.* **21,** 929 (1986).

9. T. HUGHBANKS AND R. HOFFMANN, *J. Amer. Chem. Soc.* **105,** 1150 (1983).
10. O. K. ANDERSEN, W. KLOSE, AND H. NOHL, *Phys. Rev. B* **17,** 1209 (1978).
11. W. SCHRAMM, dissertation, University of Münster (1981).
12. M. MAREZIO, P. D. DERNIER, J. P. REMEIKA, E. CORENZWIT, AND B. T. MATTHIAS, *Mater. Res. Bull.* **8,** 655 (1975).
13. R. SCHÖLLHORN, *Comments Inorg. Chem.* **2,** 271 (1983).
14. W. SCHRAMM, R. SCHÖLLHORN, H. ECKERT, AND W. MÜLLER-WARMUTH, *Mater. Res. Bull.* **18,** 1283 (1983).